A&A 496, 547–556 (2009)
DOI: 10.1051/0004-6361/200809733

Astronomy & Astrophysics

The surface of (136108) Haumea (2003 EL_{61}), the largest carbon-depleted object in the trans-Neptunian belt

N. Pinilla-Alonso[1], R. Brunetto[2,3], J. Licandro[4], R. Gil-Hutton[5], T. L. Roush[6], and G. Strazzulla[3]

[1] Fundación Galileo Galilei & Telescopio Nazionale Galileo, PO Box 565, 38700, S/C de La Palma, Tenerife, Spain
e-mail: npinilla@tng.iac.es
[2] Institut d'Astrophysique Spatiale, Université Paris-Sud, bâtiment 121, 91405 Orsay Cedex, France
[3] INAF - Osservatorio Astrofisico di Catania, via S. Sofia 78, 95123, Catania, Italy
[4] Instituto de Astrofísica de Canarias, c/vía Láctea s/n, 38205, La Laguna, Tenerife, Spain
[5] Complejo Astronómico El Leoncito (Casleo) and San Juan National University, Av. España 1512 sur, J5402DSP, San Juan, Argentina
[6] NASA Ames Research Center, MS 245-3, Moffett Field, CA 94035-1000, USA

Received 6 Mars 2008 / Accepted 14 November 2008

ABSTRACT

Context. Previously known as 2003 EL_{61}, (136108) Haumea, is the largest member of a group of trans-Neptunian objects (TNOs) with similar orbits and "unique" spectral characteristics in the form of a neutral slope in the visible and the deepest water ice absorption bands observed in the trans-Neptunian belt (TNb). Studying the surface of 2003 EL_{61} provides useful constraints of the origin of this particular group of TNOs and about the outer Solar System's history.
Aims. We attempt to study the composition of the surface of 2003 EL_{61}.
Methods. We present visible and near-infrared spectra of 2003 EL_{61} obtained with the 4.2 m WHT and the 3.6 m TNG telescopes at the "Roque de los Muchachos" Observatory (Canary Islands, Spain). Near-infrared spectra were obtained at different rotational phases covering almost one complete rotational period. Spectra are fitted using scattering models based on Hapke theory and constraints on the surface composition are derived.
Results. The observations confirm previous results that the 2003 EL_{61} spectrum is neutral in color and exhibits deep water-ice absorption bands. They also provide new facts about the surface of this object: the lack of significant variations in the spectral slope (in the near-infrared) and the depth of the water-ice absorption bands at different rotational phases clearly evident in the data, suggest that the surface of 2003 EL_{61} is homogeneous. The scattering models indicate that a 1:1 intimate mixture of crystalline and amorphous water ice is the most probable surface composition of this big TNO, and constrain the presence of other minor constituents to a maximum traction of 8%.
Conclusions. The derived composition suggests that: a) cryovolcanism is unlikely to be the resurfacing process that retains the surface of this TNO, and the other members of this population, covered mainly by water ice; b) the surface is older than 10^8 yr which constrains the timescale of any catastrophic event. such as the collision suggested to be the origin of this population, to at least 10^8 yr; c) the surface of 2003 EL_{61} is depleted of carbon-bearing species. According to the orbital parameters of the population, this implies that is a possible source of carbon-depleted, Jupiter-Family comets.

Key words. Kuiper Belt – solar system: formation – techniques: spectroscopic – astrochemistry

1. Introduction

Discovered by Santos-Sanz et al. (2005), TNO (136108) 2003 EL_{61} was classified as a dwarf-planet by the IAU and named Haumea. It is the largest member of a group of TNOs with surfaces composed of almost pure water ice that orbits the Sun in a narrow region of orbital parameter space ($41.6 < a < 43.6$ AU, $25.8 < i < 28.2$ deg., $0.10 < e < 0.19$, Pinilla-Alonso et al. 2007). Brown et al. (2007) suggested that this group is a family of fragments produced by a giant collision that occurred in the trans-Neptunian belt (TNb). The spectra of all these objects exhibit the same characteristics: they are dominated by neutral slopes in the visible and large water ice absorption bands in the near-infrared (Pinilla-Alonso et al. 2007).

Studying the surface composition of these TNOs could provide important clues in understanding the origin of this group, the role of collisions in sculpting the TNb, and the resurfacing processes that take place in this region of the Solar System. Since the discovery of this object several studies have been undertaken for these purposes.

Rabinowitz et al. (2006) presented a photometric study of 2003 EL_{61} indicating that this body has an unambiguous double-peak light curve. They discussed two different explanations of this curve: 1) the body is a homogeneous, elongated ellipsoid whose shape determines the light-curve variations; and 2) the object is a flattened spheroid whose light variations are related to albedo patterns on its surface.

Tegler et al. (2007) presented a visible spectrum of 2003 EL_{61} that was featureless, with a neutral slope. They also reported the possible existence of a band at 5773 Å probably due to O_2-ice, although the robust detection of this feature would require higher signal-to-noise ratio (S/N).

Trujillo et al. (2007) presented a near-infrared spectrum of 2003 EL_{61}. Using Hapke models, they suggested that it could be modeled using crystalline water ice and a blue component required to reproduce spectral features above 2.35 μm such as

HCN or hydrated tholins. Merlin et al. (2007) presented a new visible and near-infrared spectrum of 2003 EL_{61} and fit it with Skhuratov models. They suggested that the surface of the TNO consisted of water ice, mainly in crystalline state, in a small fraction of the surface the water ice could be amorphous.

Lacerda et al. (2008) obtained high-precision, time-resolved photometry in the visible and near-infrared. They measured there is no variation in the 1.5 μm water-ice band higher than 5%. They also detected subtle $B-R$ and $R-J$ variations with rotation that were consistent with the existence of a spot on the surface of different color and albedo from the mean surface of 2003 EL_{61}.

We present new spectroscopic observations of 2003 EL_{61} in the visible and near-infrared (Sect. 2). In Sect. 3, we present a collection of near-infrared spectra of 2003 EL_{61} taken at different rotational phases and study the homogeneity of its surface. In Sect. 4, we model the spectrum of 2003 EL_{61} and discuss the physical and compositional implications for the object. We discuss previous results in Sect. 5 and summarize our conclusions in Sect. 6.

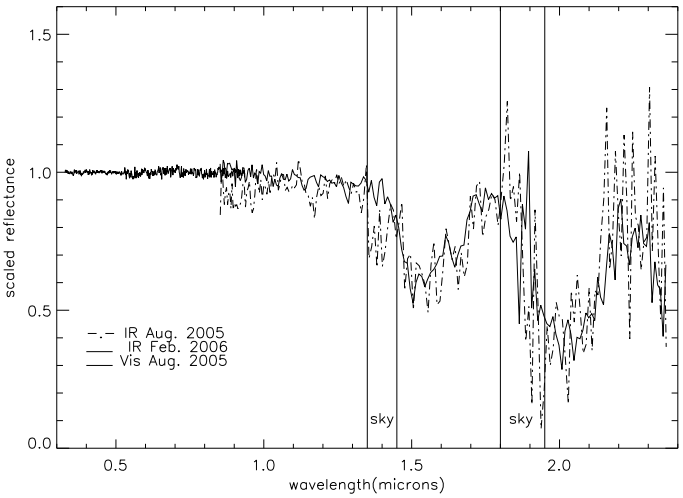

Fig. 1. VIS (2005) and NIR (2005 and 2006) spectra of 2003 EL_{61}. IR spectra match within the errors. Red slope bellow 1 μm in 2005 NIR spectrum can be a result of the centering of the object in the slit. Uncertainties are given by the point to point variation.

2. Observations

On 2005 August at 1.92 UT, we observed 2003 EL_{61} simultaneously with two telescopes at the "Roque de los Muchachos Observatory" (ORM, Canary Islands, Spain), namely the 4.2 m william herschel telescope (WHT) and the Italian 3.6 m telescopio nazionale galileo (TNG), and only in the near-infrared with the TNG on 2006 February 25, from 01:21 to 04:33 UT. Both nights were photometric.

2.1. Visible spectrum

The visible spectrum (0.35–0.98 μm) was obtained using the low resolution gratings (R300B and R158R with dispersions of 0.86 and 1.63 Å/pixel, respectively) of the double-armed spectrograph ISIS at the WHT, and a 5″ slit width oriented at the parallactic angle (the position angle for which the slit is perpendicular to the horizon) to minimize problems with differential atmospheric refraction. The tracking was at the TNO proper motion. Three 300 s spectra were obtained by shifting the object by 10″ in the slit to correct for fringing in a more accurate way. Calibration and extraction of the spectra were completed using IRAF following standard procedures (Massey et al. 1992)

The three spectra of the TNO were average-combined. Spectra of the solar-analogue star BS4486 and the G2 Landolt (SA) 107+998 (Landlot 1992) were acquired during the same night at similar airmass just before and after the TNO spectrum, and used to obtain the final reflectance spectrum of the TNO, normalized at 0.55 μm shown in Fig. 1.

2.2. Infrared spectrum

The near-infrared spectra were obtained using the high-throughput, low-resolution spectroscopic mode of the Near-Infrared Camera and Spectrometer (NICS) at the TNG, with an Amici prism disperser. This mode yields a complete 0.8–2.5 μm spectrum. We used a 1.5″ and a 0.75″ wide slit in 2005 and 2006 observations, respectively, corresponding to a spectral resolving power $R \sim 34$ and $R \sim 70$, respectively, along the spectrum. The identification of the TNO was completed by taking a series of images through the J_s filter ($\lambda_{cent} = 1.25$ μm). We identified 2003 EL_{61} as a moving object at the predicted position and with the predicted proper motion. The slit was oriented at the parallactic angle and the tracking corresponded to the TNO proper motion. We used the observing and reduction procedure described by Licandro et al. (2001).

The acquisition consisted of a series of images (3 in 2005 and 1 in 2006 observations respectively) of 90-s exposure time at one slit position (position A) and then offsetting the telescope by 10″ in the direction of the slit (position B). This process was repeated by completing several AB cycles of total exposure time of 1080 and 5220 s in 2005 and 2006, respectively.

To correct for telluric absorption and derive the relative reflectance, the G stars Landolt (SA) 98–978, Landolt (SA) 102–1081, Landolt (SA) 107–998 (Landlot 1992) were observed at different airmasses along the night, before and after the TNO observations, and used as solar analogue stars. The use of these Landolt stars as solar analogues was studied by Licandro et al. (2003). It was found that, in the near-infrared and at low spectral resolution, the spectra of these stars are similar to those of solar analogue stars and can be used in the reduction process in the same way.

The spectra of 2003 EL_{61} were divided by the spectra of the solar analogue stars, and then normalized to unity around 1.0 μm to obtain the scaled reflectance. In Fig. 1. the resulting spectra obtained by combining all the extracted AB each night and normalized to join the visible spectrum around 0.9 μm, are presented.

Around the two large telluric water band absorptions the S/N of the spectrum is very low. Even in a rather stable atmosphere, the telluric absorption can vary between the object and solar analogue observations introducing artifacts. Therefore, any spectral feature detected within the 1.35–1.46 and 1.82–1.96 μm regions cannot be considered automatically to be real. There are also a few weaker telluric absorption regions: 0.93–0.97, 1.10–1.16, 1.99–2.02, and 2.05–2.07 μm. Features in these regions must be carefully evaluated.

3. Analysis of the spectrum

The spectrum of 2003 EL_{61} presented here exhibits characteristics similar to that described previously (Merlin et al. 2007, and references therein): (a) the visible spectrum is featureless within the S/N and neutral (the spectral slope, computed

Table 1. NIR spectra information.

Spectrum[a]	Date	Texp(s)	Airmass	Rot. Phase
Aug. 2005	1.92–1.93	1080	1.90	?
2006 phase1	25.06–25.07	1080	1.30	0–0.10
2006 phase2	25.08–25.10	1080	1.19	0.13–0.32
2006 phase3	25.13–25.15	720	1.05	0.47–0.55
2006 phase4	25.15–25.17	540	1.02	0.59–0.73
2006 phase5	25.18–25.19	720	1.01	0.77–0.84

[a] We list, the name, the date, total exposure time, mean airmass, and rotational phase of the near infrared spectrum obtained in 2005 and the five combined spectra from the series obtained on 2006 February 25 (see text).

between 0.53 and 1.00 μm, is $S'_{\rm vis} = 0.0 \pm 2\%/1000$ Å); this neutral slope and the high albedo estimated for this TNO ($\rho_{\rm v}$ = 0.6–0.8, Rabinowitz et al. 2006) are indicative of the lack of complex organics (typically red in color produced by the irradiation of hydrocarbons and/or alcohols) on its surface; (b) the slope of the continuum is blue in the near-infrared; (c) the spectrum exhibits two deep absorption bands centered on 1.52 and 2.02 μm, which are indicative of water ice; (d) the band at 1.65 μm, typical of crystalline water ice, appears in all our near-infrared spectra; (e) there is a clear absorption above 2.2 μm; (f) there is no absorption band in the 0.6–0.8 μm spectral region, which would indicative of phyllosilicates (Fornasier et al. 2004).

Due to the insufficient S/N of our spectrum in the visible, we are unable to confirm the presence of a feature at ≈0.58 μm apparently detected by Tegler et al. (2007), which would be related to the presence of O_2-ice at the surface.

3.1. Rotational variation

On 2006 February 25, we obtained a series of near-infrared spectra of 2003 EL_{61} from 01:21 to 04:33 UT. The rotation period of this TNO is 3.9 h (Rabinowitz et al. 2006), so our observations monitored about 80% of the rotation of 2003 EL_{61} and allow us to investigate the presence of possible surface inhomogeneities. We combined five subsamples of this series to produce five spectra covering different rotational phases (see Table 1 for details). Figure 2 presents these five spectra and the spectrum obtained in 2005.

There is no evidence of large inhomogeneities on the surface of the TNO. Every single spectrum shows the same features. Figure 3 shows the ratio of these spectra to the spectrum of 2003 EL_{61} represented in Fig. 1 (labeled *sp2006all*). We note that there is no systematic deviation within the limits of the noise for none of the spectra obtained at different phases, neither in the slope nor for the different spectral bands.

Finally, to quantify any possible variation in the slope and/or band depths of the spectra, we computed two parameters:

(a) the normalized infrared reflectivity gradient $S'_{\rm ir}$[%/1000 Å] over the 0.85–1.3 μm range. To compute this, we fit the continuum between 0.85 and 1.3 μm with a straight line. This fit is sensitive to the first and last points of the spectrum but the error introduced by this factor is negligible compared with the systematic errors.

(b) the depth of the bands, D, with respect to the continuum of the spectrum (fitted in the infrared using a cubic spline) given by $D = 1 - R_{\rm b}/R_{\rm c}$, where $R_{\rm b}$ is the reflectance in the center of the band (1.52 or 2.02 μm) and $R_{\rm c}$ is the reflectance of the continuum at the same points (1.52 or 2.02 μm, respectively).

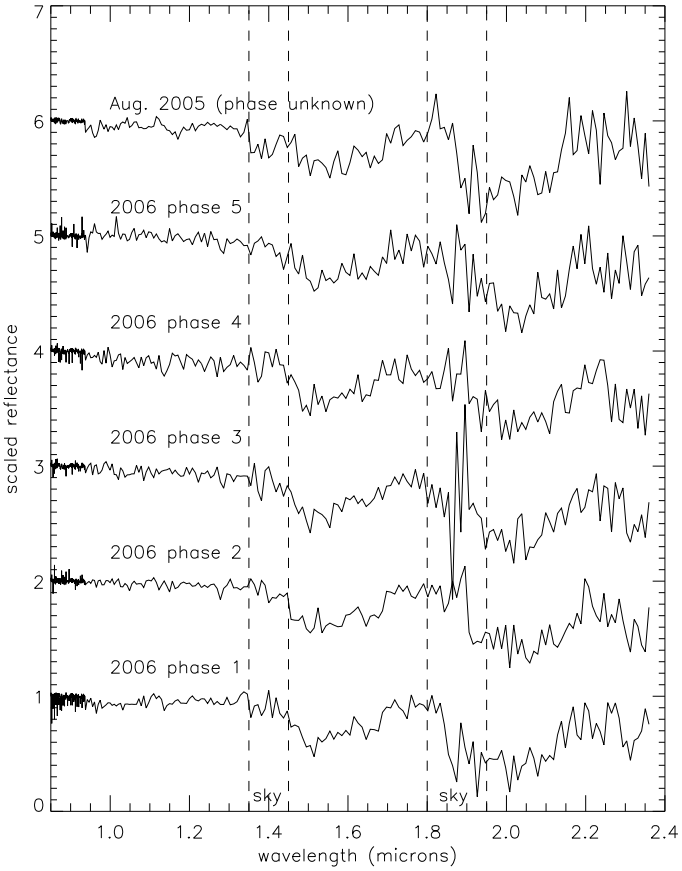

Fig. 2. Five spectra obtained on 2006 February 25 covering different rotational phases (see text for details) and the spectrum obtained in 2005. Uncertainties correspond to the point to point variations. Notice that all spectra are similar suggesting that the surface is homogeneous to within our errors (see text for more details).

Table 2 presents the parameter values derived for each spectrum. The mean $S'_{\rm ir} = -0.9 \pm 1.8$. The largest deviation from this mean value corresponds to the spectrum obtained at phase 1 and is 2.5%/1000 Å. Considering that, due to systematic errors (e.g. centering uncertainties in the TNO and/or solar analogues in the slit), uncertainties of 2%/1000 Å in the slope are usual, we should conclude that the spectral slope is similar at all rotational phases. Lacerda et al. (2008) found a small variation of 0.035 mag in the $B - R$ color of 2003 EL_{61} correlated with the rotation of the TNO. They suggested that this was produced by a region of the surface of lower albedo that was redder in color. This change in color corresponds to a reddening in S' of about 1–2%/1000 Å, which is smaller than the uncertainties in our measurements, so we are unable to confirm 2008 results from the study of the spectra.

In the same way, the mean depth of the water absorption bands $D_{1.52}$ and $D_{2.02}$ are 33.7 ± 2.5 and 53.5 ± 4.0 respectively. The errors in the measured band depths for each spectrum are larger than the deviation from the mean, so we can conclude that there are no variations in the depths of the water absorption bands larger than 7%. We conclude that, to within the limitations of the signal-to-noise ratio of our observations, the surface of 2003 EL_{61} is homogeneous. This reinforces the hypothesis that its shape is an elongated ellipsoid.

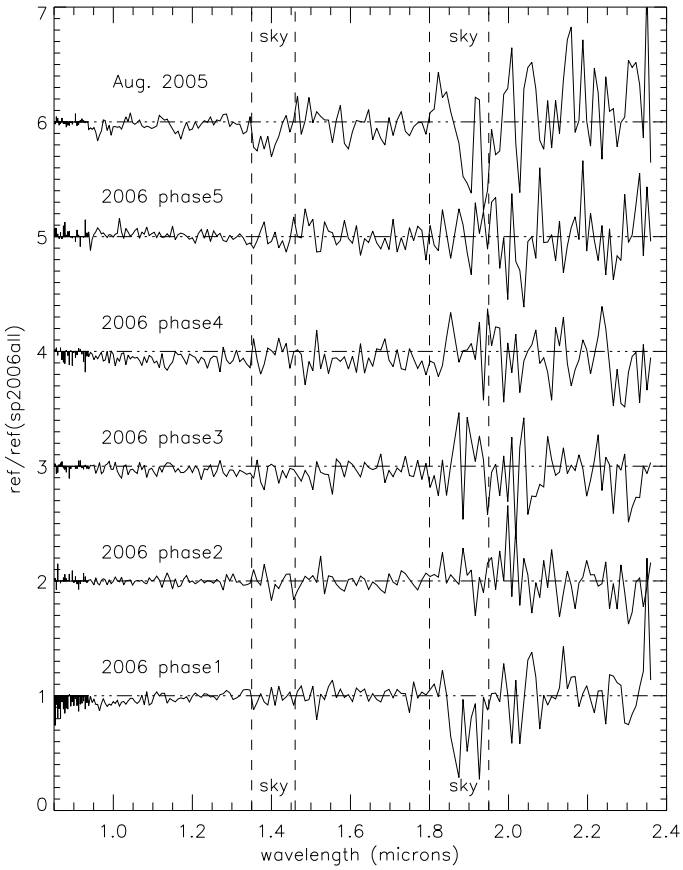

Fig. 3. Ratio between the spectra shown in Fig. 2 and the *sp2006all* spectrum. Uncertainties are given by the point of point variation. Notice that there is no systematic deviation within the limit of the noise for none of the spectra obtained at different phases.

Table 2. Normalized reflectivity gradient S'_{ir} and depth of the 1.52 and 2.02 μm bands D, as defined in the text, for all the considered infrared spectra.

Name	[a] S'_{ir}	$D_{1.52}$	[b] $\varepsilon_{1.52}$	$D_{2.02}$	[b] $\varepsilon_{2.02}$
Aug. 2005	1.07	31.13	7.2	49.7	13.5
sp 2006all	–1.40	34.0	4.8	53.8	6.6
2006 phase1	1.61	33.9	6.7	55.8	10.0
2006 phase2	–1.77	33.3	5.6	51.3	10.2
2006 phase3	–2.12	38.3	7.0	54.6	10.6
2006 phase4	–2.32	32.4	9.2	49.5	13
2006 phase5	–1.97	33.1	7.8	59.8	10.6

[a] Uncertainties of 2%/1000 Å in the slope are typical due to systematic errors (see text for details); [b] ε are the errors associated with D.

4. Spectral models

We use the Hapke scattering model (Hapke 1981; Hapke 1993) to reproduce the spectrum of 2003 EL_{61} and derive conclusions about its surface composition. In particular, we test whether the spectrum is consistent with the presence of amorphous ice and investigate the presence of other minor components.

To reproduce the model, we use our spectrum of the best S/N, named *sp2006all*, obtained by combining all our spectra acquired in the 2006 run as explained in Sect. 2. To increase the S/N of the spectrum in the near-infrared, we merged our spectrum of 2003 EL_{61} with that of Trujillo et al. (2007). Hereafter we refer to this *"composite spectrum"* as the spectrum of 2003 EL_{61} and refer to *sp2006all* as *"our spectrum"*. As discussed above, there are no significant differences between our spectrum, the composite spectrum, and the other published data.

The synthetic spectra that we show are obtained by fitting the composite spectrum of 2003 EL_{61} using the relative reflectance scaled at visible wavelengths. The free parameters in this fitting procedure are the relative abundances and grain sizes of the various components. After completion of the fitting procedure, the resulting abundances and grain sizes are used in a separate procedure that uses the same optical constants to calculate the geometric albedo.

The shape and position of the bands for crystalline water ice is dependent on several factors, for example the temperature of the ices or the abundance and sizes of the particles. For each configuration, an automatic algorithm varied the abundances and grain sizes for each of the materials and attempted to reproduce the spectrum. We tested, when available, with optical constants at different temperatures so to chose the most appropriate. The models we show are always the ones corresponding with the smallest value of the reduced chi-squared value for each assumed composition.

We emphasize that knowledge of the optical constants is often poor, which affects both the calculation and the model results. Thus, from visible and near-infrared observations it is usually impossible to retrieve a unique composition, and the fits that we show sould be regarded as possible solutions.

For crystalline water ice, we use optical constants from Grundy & Schmitt (1998, obtained at $T = 40$ K) in the 1.0–2.5 μm spectral region and from Warren (1984) (obtained at $T \approx 266$ K) at shorter wavelengths. Unfortunately, no data are available at appropriate temperatures in the visible region. The intensity of the 1.65 μm band that characterizes crystalline ice depends on the temperature, being higher at lower T. In Sects. 4.1 and 4.2, we tested fits with water ice at temperatures between 30 K and 80 K, which is possible only for crystalline water ice (Grundy & Schmitt 1998) due to the small amount of optical constants available. In all cases, the use of optical constants at 40 K seems more appropriate for TNOs. However we emphasizes that ice formed directly at 40 K is amorphous and does not exhibit the 1.65 μm band. The observation of the crystalline form then implies that ice present on 2003 EL_{61} experienced higher temperatures (e.g. Baratta et al. 1991). For amorphous water ice, we use optical constants from Schmitt et al. (1998, obtained at $T = 38$ K) in the near-infrared and those of crystalline water ice from Warren (1984) at wavelengths shorter than 1 μm because, to the best or our knowledge, no optical constants for amorphous ice are available in this spectral region.

We emphasize that ion irradiation produces amorphous ice that is similar to deposited amorphous ice (Leto & Baratta 2003), and this allows us to use optical constants of deposited amorphous ice to mimic the amorphization induced by cosmic rays on TNOs. However, differences may be present, so future studies should focus on the derivation of optical constants of irradiated ice.

In this paper, we also attempt to reporduce data with models by considering the following minor components, CH_4, polyHCN, NH_3, Ammonia Hydrate, Kaolinite, and Ortho-Pyroxene, for which we use the optical constants from Grundy et al. (2002), Khare et al. (1994), Sill et al. 1980), Brown et al. (1988), Clark et al. (1981), and Brunetto et al. (2007), respectively.

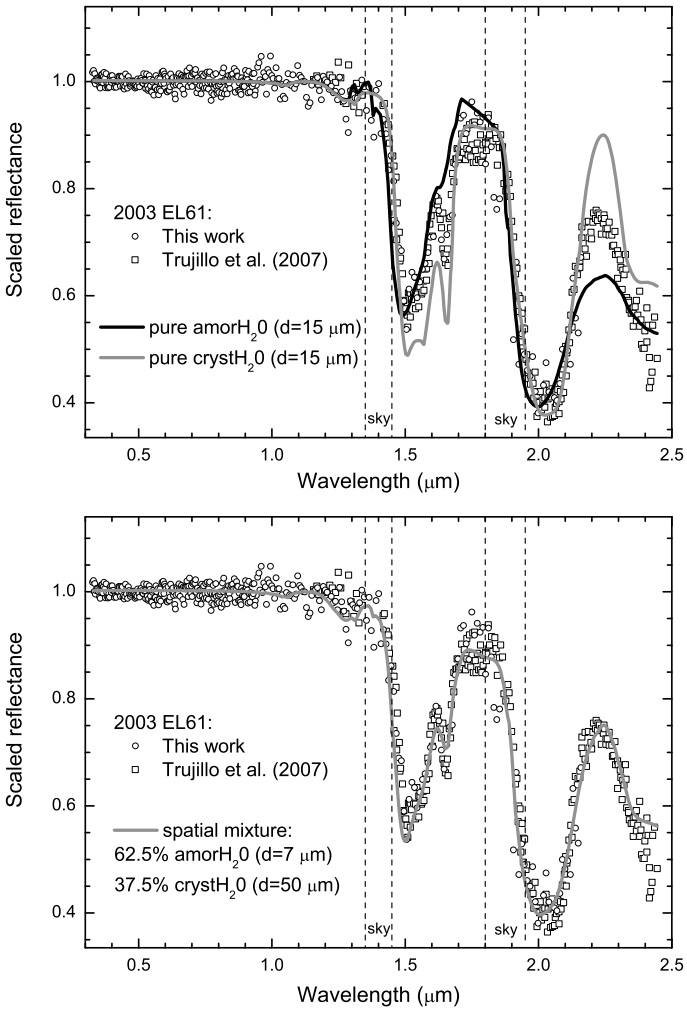

Fig. 4. *Upper panel*: the composite spectrum of 2003 EL_{61} compared with two synthetic spectra, using only crystalline or only amorphous water ice. *Lower panel*: the composite spectrum of 2003 EL_{61} fitted by a spatial mixture of crystalline and amorphous ice; either trials, the fit is not satisfactory especially around 1.65 μm .

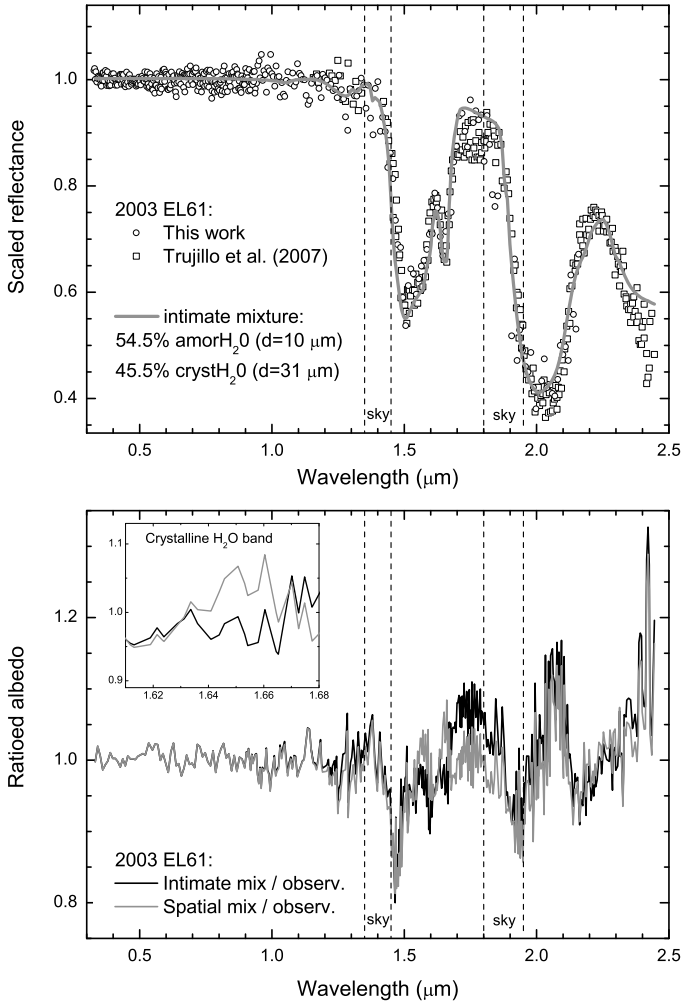

Fig. 5. *Upper panel*: the composite spectrum of 2003 EL_{61} fitted by an intimate mixture of crystalline and amorphous ice. *Lower panel*: ratio of the spatial to intimate mixture models, and the composite spectrum; the regions for which discrepancies appear are evident. The insert shows the region of the 1.65 μm feature, where an intimate mixture clearly provides a more accurate description of the data as confirmed by the reduced chi squared value of the fit.

4.1. Crystalline and amorphous water ice spatial mixtures

We first attempted to reproduce the *composite spectrum* with pure crystalline water ice at 40 K (Fig. 4, upper panel), although our fit was unable to reproduce the 1.52– and 2.02-μm bands and at a decrease in reflectance at wavelengths ≥2.2 μm band. We tested a few additional models by considering crystalline ice temperatures of up to 80 K, although we were unable to reproduce the spectrum of 2003 EL_{61}. We investigated the possibility of reproducing the spectrum with only pure amorphous water ice (Fig. 4. upper panel). Because the 1.65 μm feature is absent in amorphous ice reflectance, models of this pure material do not reproduce the spectrum of EL_{61} well either. Additionally, the 2 μm band minimum of amorphous ice occurs at too short a wavelength when compared with the observations.

We then investigated a model of a mixture of amorphous and crystalline ice. We initially assumed that crystalline and amorphous ice are spatially segregated on the surface and the results are shown in the lower panel of Fig. 4. The best-fit solution is a model of two segregated components: 37.5% of crystalline water ice (with grain size of 7 μm) and 62.5% of amorphous water ice (with grain size of 50 μm). In the visible range, the mixture produces a flat spectrum and a geometric albedo of about 0.7, which agrees with previous estimations (Rabinowitz et al. 2006).

The fit curve is not entirely satisfactory because, even if several features of the spectrum are well reproduced, it is unable to reproduce the depth of the 1.65 μm band.

4.2. Crystalline and amorphous water ice intimate mixtures

Since the spatial mixture was unsatisfactory, we tested some intimate mixtures of amorphous and crystalline ice. The best result is shown in the upper panel of Fig. 5; the model corresponds to a 54.5% of amorphous ice (grain size of 10 μm) and a 45.5% of crystalline ice (grain size of 31 μm). This model produces slightly different grain sizes for amorphous and crystalline ice but considering the uncertainties in the optical constants the differences in size may be insignificant. In the visible range, our model produces a flat spectrum and a geometric albedo of about 0.7.

The reduced χ^2 value for this model is 3 for both the intimate and spatial models if we include the entire spectrum. However, if we restrict the χ^2 analysis to the region about 1.65 μm, where the

band of crystalline water ice is centered, the intimate mixture reproduces the composite spectrum more accurately than the spatial mixture (see Fig. 5, lower panel) as confirmed by a χ^2 of 3 for a spatial mixture and 2.4 for an intimate mixture. However, the quality of the fit in the 1.7–1.85 μm range is reduced. In the 1.7–1.85 μm range, the uncertainties in the optical constants are larger than in the 1.65 μm spectral band because the absorbance of the water ice is almost zero. Some discrepancies are still present in the 2.2 μm to 2.4 μm region. These discrepancies appear systematically in all our models. It is useful to remind the reader that the broad-band color of amorphous water-ice reflectance is not well-constrained by laboratory experiments, due in part to grain-sized effects, and the difficulty in obtaining optically thick samples of amorphous water ice. Additionally, these discrepancies may be attributed to uncertainties in the optical constants of amorphous water ice.

We also included models using multiple grain sizes, using up to 3 components for both amorphous and crystalline ice, i.e. a 6-component set, but the spectral fit was not improved. Thus, the 2-component model provides a reliable and relatively simple description of the TNO's surface. One implication of an intimate mixture of crystalline and amorphous water ice is a homogeneous surface, which is consistent with our results for the rotational-variation observations.

From our models, we can estimate that the fraction of amorphous water ice with respect to the total water (amorphous + crystalline) abundance on the surface of 2003 EL_{61} is in the range 0.45–0.65. This would correspond to a minimum and maximum fraction of crystalline/amorphous H_2O of about 0.54 and 1.22, respectively. The 1:1 ratio is used in the text as a convenient means of representing the relative abundances to within the uncertainties of the models.

A model that considers an intimate mixture of amorphous and crystalline water ice was first proposed by Merlin et al. (2007). Comparing our fit with that of Merlin et al. (2007) we are able to achieve more reliable results in the region of the main features (1.52, 1.65, 2.02 μm). Compositionally, our models providea far higher percentage of amorphous ice. The ratio of amorphous to crystalline water ice is related to the time that the ice has been exposed to irradiation (Leto et al. 2003 & Strazzula et al. 2003), so this result can be helpful in estimatign the age of the surface of 2003 EL_{61}, as we discuss later. Merlin et al. (2007) used grain sizes for amorphous and crystalline ice that differed by more than a factor of 10, which is very difficult to account for, while in our model the difference decreases to a factor of 3. The difference between our model and that of Merlin et al. (2007) is that theirs included a small amount of amorphous carbon. We study this in the section dedicated to minor components.

We conclude that we were able to reproduce the spectrum of 2003 EL_{61} accurately and with more robust physical meaning than previous fits by assuming an amorphous/crystalline ratio of 1:1 that is indicative of competition between different physical processes on the surface.

4.3. Layered models

Although not yet fully explored, one option that the Hapke model offers is a layered system (e.g. Brunetto & Roush 2008). We use Eqs. (7.45c), (8.89), (9.14), and (11.24) from Hapke (1993) in a model that calculates the reflectance from a system where a layer is located above an infinitely thick substrate.

This physical model arises from the consideration that 2003 EL_{61} is irradiated by solar wind and cosmic ions. Given this situation, it is reasonable to imagine that a layer of ice close to the surface has suffered a dose of irradiation that decreases with increasing depth causing the amorphization of water ice.

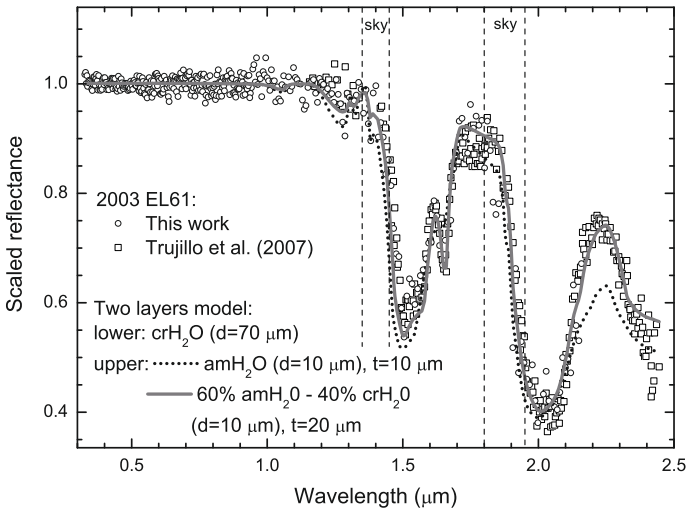

Fig. 6. Multi-layer models for 2003 EL_{61}: amorphous ice on top of crystalline (dot) provides an unsatisfactory, while an intimate mixture of amorphous and crystalline ice on top of crystalline (solid) is more appropriate description of the data. Upper layer thickness and grain sizes are given for each model.

We initially considered a configuration where an amorphous mantle is on top of a crystalline substrate (Fig. 6, dotted curve). Our result, however, were unsastisfactory, because the use of only an upper layer of 10 μm amorphouse ice is sufficient to reduce the 1.65 μm band of the underlying crystalline ice, below that seen in the observations of 2003 EL_{61}.

We then considered a configuration where the upper layer consists of an intimate mixture of amorphous and crystalline water ice (Fig. 6, solid curve). This model consists of an intimate mixture of 60% amorphous and 40% crystalline ice, on top of an infinite crystalline-ice substrate, and it provides a closer description of the data.

However, as for the intimate and spatial mixtures, there are some remaining differences between the model and the spectrum, especially in the 2.2 to 2.4 μm spectral range. As discussed above, these may arise due to the uncertainties in the optical constants, especially of amorphous water ice.

We find that all three major models (spatial mixture, intimate mixture, two-layers model) produce reduced χ^2 values of $\approx$3. This would not allow us to differentiate between the various physical representations of the surface. However, if we restrict the analysis to the region of the 1.65 μm feature, we find values of 3, 2.4, and 1.8 for the spatial, intimate, two-layer models, respectively. These simple tests indicate that layered models can be a useful tool for interpreting TNOs spectra. Future efforts should focus on the possibility of modeling several layers, since ion irradiation would affect the icy layers gradually, and a sudden transition from amorphous to crystalline is unexpected.

4.4. Minor components

One of the aims of this paper is to place constraints on the presence of minor components on the surface of 2003 EL_{61}. We investigated the contribution of some species, using them as minor components in an intimate mixtures of amorphous and crystalline water ice. We consequently estimated upper limits for these species, and the results are included in Table 3.

Table 3. Upper limits for possible minor components of the surface of 2003 EL_{61}.

Species	Upper limit	Species	Upper limit
NH_3	5%	serpentine	7%
poly-HCN	5%	kaolinite	4%
CH_4	5%	orthopyroxene	7%
CO_2	6%	olivine	5%
NH_4OH	8%		

We included in particular materials proposed to exist on the surface of 2003 EL_61. We found that none of these components improved the fit quality (see Fig. 7). Even small amounts of these materials altered the shape of the model function by adding spurious features or reddening the slope, and hence decreasing the quality of the fit.

The presence of ≥5% ammonia and methane introduced features in the 2.2–2.3 μm region that are inconsistent with the observations (models A and C respectively).

The serpentine (not shown) and kaolinite contribution could help to produce a blue slope in the long wavelength region, but using percentages higher that 5–10% introduces other features (especially in the visible, model D in Fig. 7) that are not present in the observations. The large contribution of another silicate, pyroxene, (model E in Fig. 7), is discanot considered also because a small percentage of 7% would be sufficient to introduce a broad feature in the visible spectrum between 0.8 and 1.1 μm.

A simple 5% contribution of poly-HCN (model B in Fig. 7) is sufficient to produce non-neutral slopes in the visible range, which is in complete disagreement with the observations. Thus, the hypothesis of Trujillo et al. (2007) of a strong contribution of these species has to be discarded.

The presence of ammonia hydrate (model F in Fig. 7) is particularly interesting because it has been related to cryovolcanism (Jewitt & Luu 2004). We find that 8% of ammonia hydrate reduces the quality of the fit significantly. Additionally, there is no evidence of an absorption feature at 2.2 μm, associated with ammonia hydrate, in our spectrum.

Finally, we tested a few models with amorphous carbon, using the same optical constants as Merlin et al. (2007), i.e. those from Zubko et al. (1996). We investigated both intimate and spatial mixture models (see Fig. 8, upper panel for intimate mixtures, lower panel for spatial mixtures) and, in general, we found that the use of amorphous carbon did not improve the fit.

To better constrain the amount of carbon, we produced a few synthetic spectra (Fig. 8). In these spectra, we assumed that the relative percentage and grain sizes of amorphous and crystalline water ice were the values given in Fig. 5, and we gradually increased the amount of the carbon contaminant. The models are presented in terms of geometric albedo. The albedo of 2003 EL_{61} is fixed at 0.7 (open diamond) with an error bar of 0.1 as estimated by Rabinowitz et al. (2006). The grain size of carbon is fixed at 15 μm; as already noted by Merlin et al. (2007), the size of carbon particles cannot be properly constrained.

From these models results, we can infer that, in the case of intimate mixtures, a 1% carbon fraction is sufficient to force the model to disagree with the observations close to 2.2 μm even if the visual geometric albedo is consistent with the estimated albedo of the object (Rabinowitz et al. 2006). A model with a slightly larger amount of amorphous carbon, 3%, provides a visual geometric albedo that is clearly beyond the margins of error for the data of 2003 EL_61. We conclude that the amount of carbon on the surface of 2003 EL_{61} intimately mixed with water is easily ≤3%. In the case of spatial mixtures, we can derive an upper limit of ≤5% carbon, as again this quantity forces the model to disagree with the observations close to 2.2 μm, even while the visual geometric albedo is consistent with the estimated albedo of the object. A model with a higher proportion of carbon (e.g. 15%) provides an example of when even the visual geometric albedo is beyond the amrgins of error of the object. The reduced χ^2-values for the 3% (intimate mixture) and 5% (spatial mixture) models are about 8 and 4, respectively, and both values are higher than the values found for models with pure water ice, (~3).

Appart from water ice, we discard the major presence of other components on the surface at a high level of confidence. We emphasize that none of the components investigated helped to improve the fit quality. In particular, the main discrepancies for the spectral range of 2.2–2.4 μm remain.

5. Discussion

We have measured a surface composition of >92% of pure water ice for 2003 EL_{61} and demonstrated that the presence of a significant fraction of complex organics on its surface would be inconsistent with the observational data. TNOs with no traces of organics should be uncommon. If the original chemical composition of all TNOs is similar i.e. objects consist of an abundant ammount of water ice with molecular ices such as CO, CO_2, CH_4 and N_2, then laboratory experiments with astrophysical ice mixtures containing hydrocarbons show that long term processing by high energy particles and solar radiation induces the loss of hydrogen and the formation of complex organic species, resulting in dark and usually red materials (Moore et al. 1983; Johnson et al. 1984; Strazzulla & Johnson 1991). In the case of a TNO, Gil-Hutton (2002) demonstrated that the timescale required to form carbon residue, accounting for the competition between darkening by cosmic-rays and resurfacing due to impacts, is ~10^9 years. Given this timescale, it is expected that a normal TNO begins to show the reddening of its spectrum on shorter timescales.

As previously proposed for 2005 RR_{43} (Pinilla-Alonso et al. 2007), one member of the group, different scenarios can explain their surface composition: the surface can be replenished with relatively fresh material (e.g. due to cryovolcanism, multiple collisions or a recent huge collision), or these objects can be originally carbon-depleted.

Replenishment of fresh surface material can be explained by the emergence of of unaltered material from the interior. Subsurface material could be exposed by outgassing or flows from the interior produced by cryovolcanism. This process would produce a surface consisting of patches of fresh water ice partially covering an older surface of processed ices. Cryovolcanism was proposed as a menas of continuously resurfacing the surface of medium-size TNOs (Stevenson 2004) but has always been related to ammonia hydrate. Cook et al. (2007) claimed a clear detection of this material on Charon's surface. Its presence was even proposed on (50 000) Quaoar (Jewitt & Luu 2004), although this detection remains controversial (Schaller & Brown 2007). For TNOs >400 km in diameter, an ice mixture of ammonia and water would be melted at the temperatures that are typical of the interiors of these bodies. This melted mixture could propagate through cracks until reaching the surface in a similar way that basaltic volcanism propagates througth Earth (Stevenson 2004). The spectral signature of ammonia hydrate includes an absorption band at ~2.2 μm, which is not present in the spectrum of 2003 EL_{61}. Additionally, our compositional

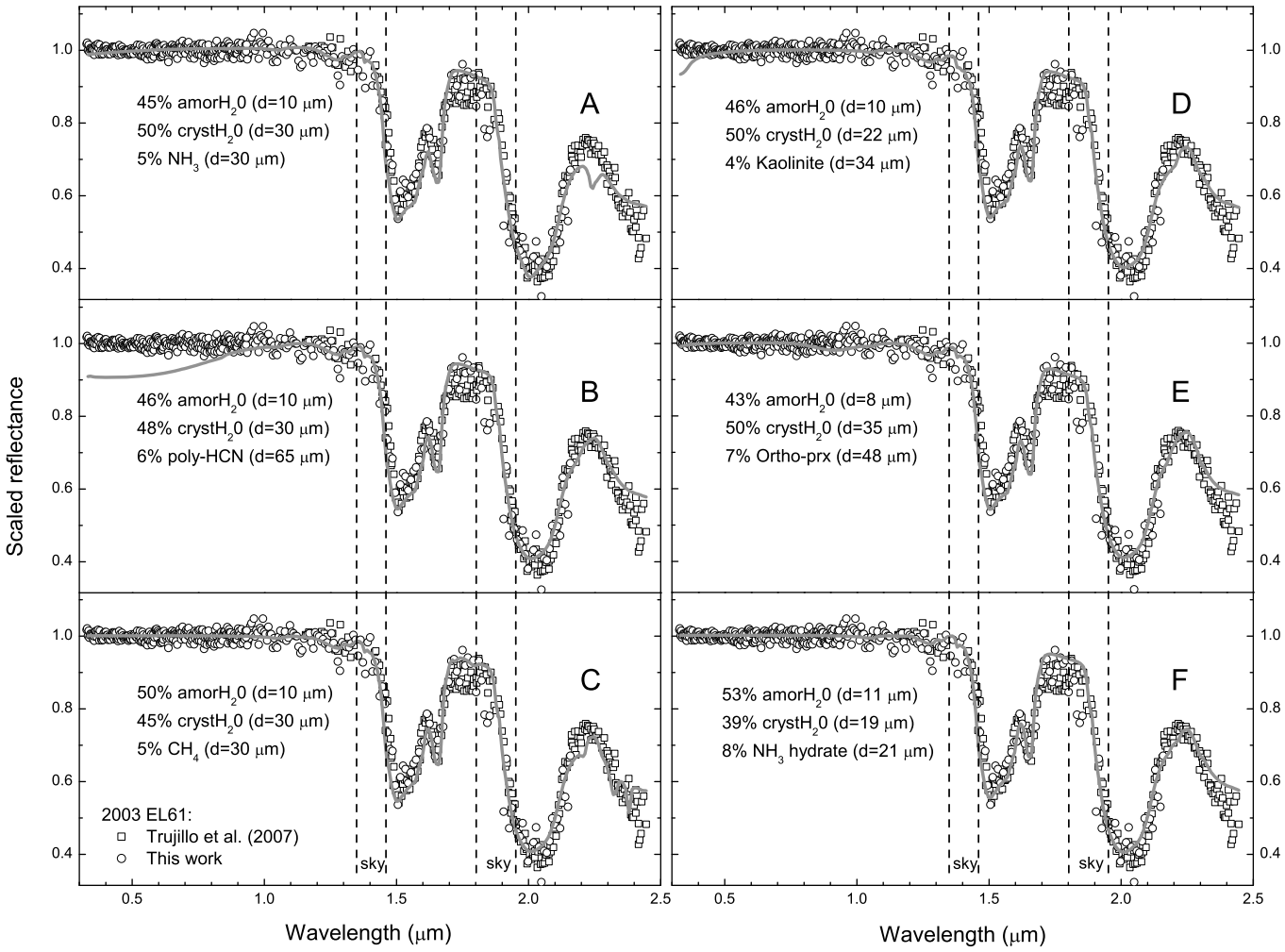

Fig. 7. The effects of including minor components in the fit of the 2003 EL_{61} composite spectrum.

models favor an intimate mixture instead of an areal one. So, unless cryovolcanism was sufficiently extensive to resurface the entire body, this process is inconsistent with the observations. Furthermore, since the surface properties of the group of TNOs related to 2003 EL_{61} are similar, we should conclude that the resurfacing mechanism acting on them is similar. However, since several have diameters <400 km, we can exclude the process of cryovolcanism.

Another scenario is that of resurfacing produced by collisions. A single collisional event was proposed by Brown et al. (2007) to be the origin of the group of TNOs related to 2003 EL_{61}. Such a massive impact would release a large amount of energy that could be converted partially into heat and produce a significant increase in the temperature (>100–130 K) leading to the crystallization of a large amount of the water ice. The eroded material would be sublimated and globally distributed over the TNO surface on a timescale of tens of hours (Stern 2002). The result of this process would be a fresh surface globally covered with crystalline water ice as proposed for 2002 TX_{300} (Licandro et al. 2006), another member of the group. After the event, the temperature of the ice would cool to about 40 K and the irradiation process would begin to transform crystalline into amorphous water ice. The ratio of amorphous to crystalline water ice on the surface of the body would enable the time elapsed since the impact to be estimated.

From our models, we infer that the ratio of amorphous water ice to total water (amorphous + crystalline) on the surface of 2003 EL_{61} is in the range 0.45–0.65. This fact can be used to constrain the age of its surface. From Fig. 9 of Leto & Baratta (2003), we can infer that this ratio corresponds to irradiating crystalline ice with a dose of 0.4–2 eV per H_2O molecule, i.e. about 1 eV per molecule with an error corresponding to an uncertainty of a factor of 2.

From Fig. 6 of Strazzulla et al. (2003), we infer that a dose of 1 eV per molecule would accumulate at 40 AU in about 5×10^7–2×10^8 years (considering surface depths between 1 μm and 1 cm), i.e. about 10^8 years with an error corresponding to an uncertainty of a factor of 2. Thus, combining the previous estimates, we can estimate a timescale of about 10^8 years with an error of a factor of 5. Continuous collisions with smaller particles in the TNb cause the recrystallization of water ice on the surface and compete with amorphization due to irradiation (Gil-Hutton 2002). So, the timescale needed to produce a 1:1 crystalline/amorphous surface is probably $>10^8$ yr.

This estimate constrains the age of the surface of 2003 EL_{61}. A recent ($<10^8$ yr) impact that rejuvenated and recrystallized the entire surface must be excluded since the data show evidence of a certain amount of amorphous water ice on the surface of 2003 EL_{61}. From the observations, we are unable to determine

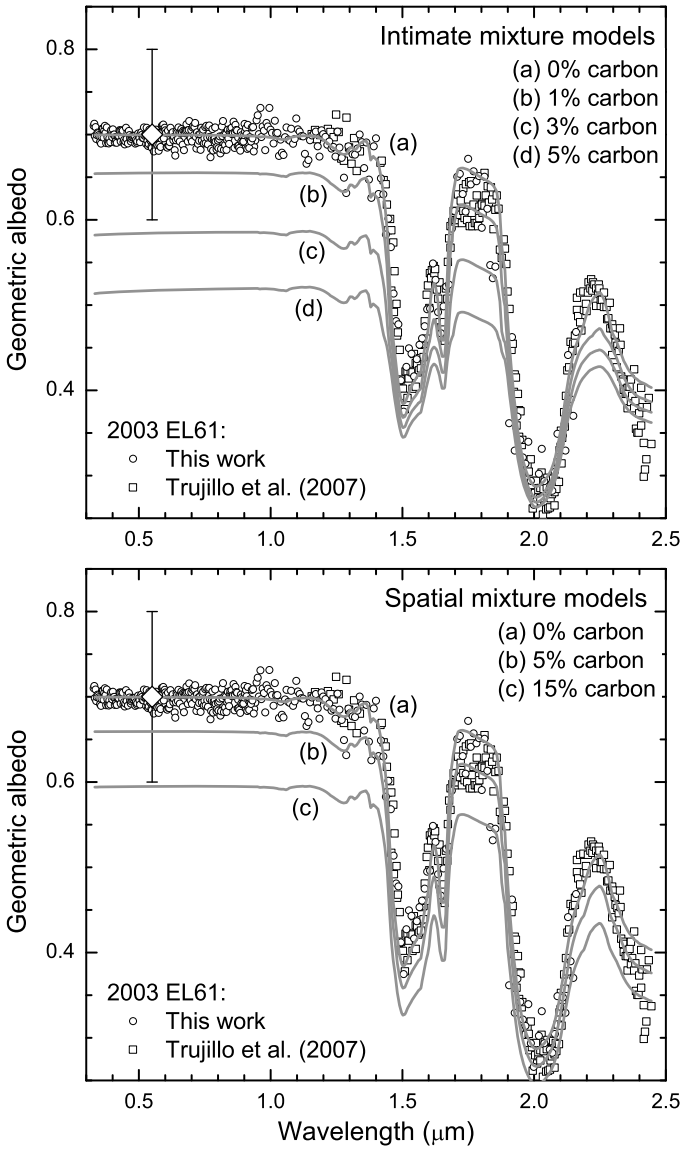

Fig. 8. Effect of adding Amorphous Carbon to the surface of 2003 EL_{61}. *Lower panel*: spatial mixture of different amounts of amorphous carbon and water ice. *Upper panel*: intimate mixture of amorphous carbon and water ice. In both cases, the relative percentage and sizes of amorphous and crystalline water ice are the same as in Fig. 5.

whether carbon depletion is related to a different original composition or to a catastrophic event that occurred on a timescale $>10^8$ yr. However, if the latter were the case, our estimate of the surface age would agree with recent calculations indicating that the large impact that most probably created the family of 2003 EL_{61} should be primordial (Ragozzine & Brown 2007).

In all cases, the surface of 2003 EL_{61} is sufficiently old, $>10^8$ yr, for complex organics to be formed on the surface. Yet, this does not appear to be the case for 2003 EL_{61} or the other objects in the group. The only possible explanation of this fact is that these body surfaces are carbon-depleted with respect to the surfaces of "normal" TNOs. In addition, for the smaller objects in this group, for which differentiation is unexpected, the depletion in carbon species must affect the global composition of the bodies.

All members of this group have similar orbital parameters, in a region crossed by the 12:7 mean motion resonance with Neptune (Nesvorný & Roig 2001). Brown et al. (2007) and Ragozzine & Brown (2007) demonstrated that fragments captured in this resonance could experience significant variations in eccentricity due to chaotic diffusion, reaching higher-eccentricity orbits. In this scenario, it is possible for several fragments to reach orbits that produce close encounters with Neptune, injecting carbon-depleted objects into the inner regions of the Solar System as Jupiter Family Comets (JFC). Since the smaller fragments of the collisional family are probably globally carbon-depleted, these objects could be a source of the comet group with similar compositional properties first suggested by A'Hearn et al. (1995).

6. Conclusions

We observed 2003 EL_{61} in August, 2005, simultaneously in the visible and near-infrared with two telescopes, the 4.2 m WHT and the 3.6 m TNG at the ORM (Canary Islands, Spain), and in the near-infrared with the TNG in February 2006. We have presented the low-resolution spectra obtained in both nights. The similarities between the near-infrared spectra obtained at different rotational phases (covering ~80% of the rotational period) imply that the surface of this TNO is homogeneous to within the margins of errors of the observations. By fitting the 2003 EL_{61} spectrum using Hapke (1981, 1993) models, we concluded that its surface is composed almost entirely of pure water ice, ≥92%. We were able to reproduce the spectrum with an intimate mixture of crystalline and amorphous water ice in the proportion 1:1. We also obtained a good fit with a layered model representing a thin cap of an intimate mixture of crystalline and amorphous water ice in the proportion of 4:6 over an infinite layer of crystalline water ice. Both configurations are physically consistent with the surface homogeneity and the processing of water ice under cosmic irradiation.

If the present surface of 2003 EL_{61} is the product of a large collision, then the ratio of amorphous and crystalline water ice that we obtain from the models implies that this collision should have ocurred more than 10^8 years ago, in agreement with dynamical models.

Furthermore, these models have enabled us to show that by adding other constituents at a level of >8%, the quality of the fit is reduced dueto the introduction of new features or the reddening of the slope in the visible range. Therefore, apart from water ice, the presence of significant amounts of other components is inconsistent with the observations. In particular, we discard the presence of complex organics at the level of >5%.

The best-fit models favor an intimate 1:1 mixture of amorphous/crystalline water ice, and no clear signature of ammonia hydrate in the spectrum. This suggests that cryovolcanism is unlikely to be the main resurfacing mechanisms on 2003 EL_{61}.

Given the estimation of age and the dearth of complex organics on the surface of 2003 EL_{61}, we conclude that, as for 2005 RR_{43}, and probably the other members of the EL_{61} group of TNOs identified by Pinilla et al. (2007), the surface of EL_{61} is carbon-depleted. In addition, the smaller members of the group, for which differentiation is unexpected, are probably globally carbon-depleted. Considering their orbital parameters, this group of carbon-depleted TNOs could be the origin of some of the carbon-depleted comets previously identified by A'Hearn et al. (1995).

Acknowledgements. Based on observations made with the Italian Telescopio Nazionale Galileo (TNG) operated on the island of La Palma by the Fundación Galileo Galilei of the INAF (Istituto Nazionale di Astrofisica) at the Spanish Observatorio del Roque de los Muchachos of the Instituto de Astrofísica de Canarias. R.B and G.S are greatful to Italian Space Agency contract

n. 1/015/07/0. T.L.R acknowledges support from NASA's Planetary Geology and Geophysics program. We acknowledge F. Merlin and S. C. Tegler for sending us their spectra of 2003 EL_{61}.

References

A'Hearn, M. F., Millis, R. L., Schleicher, D. G., et al. 1995, Icarus, 118, 223
Baratta, G. A., Leto, G., Spinella, F., et al. 1991, A&A, 252, 421
Brown, R. H., Cruikshank, D. P., Tokunaga, A. T., et al. 1988, Icarus, 74, 262
Brown, M. E., Barkume, K. M., Ragozinne, D., et al. 2007, Nature, 446, 294
Brunetto, R., Barucci, M. A., Dotto, E., & Strazzulla, G. 2006, ApJ, 644, 646
Brunetto, R., Roush, T. L., Marra, A. C., & Orofino, V. 2007, Icarus, 191, 381
Brunetto, R., & Roush, T. L. 2008, A&A, 481, 879
Clark, R. N., J. Geophys. Res. 86, 3074
Cook, J. C., Desch, S. J., Roush, T. L., et al. 2007, ApJ, 663, 1406
Cruikshank, D. P., Allamandola, L. J., Hartmann, W. K., et al. 1991, Icarus, 94, 345
Fornasier, S., Dotto, E., Barucci, A., et al. 2004, A&A, 422, 43
Gil-Hutton, R. 2002, P&SS, 50, 57
Grundy, W. M., & Schmidtt, B. 1998, JGR, 103, 25809
Grundy, W. M., Schmitt, B., & Quirico, E. 2002, Icarus, 155, 486
Hapke, B. 1981, J. Geophys. Res., 86, 3039
Hapke, B. 1993, Theory of Reflectance and Emittance Spectroscopy (New York: Cambridge Univ. Press)
Jewitt, D. C., & Luu, J. 2004, Nature, 432, 731
Johnson, R., Lanzerotti, L., & Brown, W. 1984, Adv. Space Res. 4, 41
Khare, B. N., Sagan, C., Thompson, W. R., et al. 1994, Can. J. Chem., 72, 678
Landolt, A. 1992, AJ, 104, 340
Leto, G., & Baratta, G. A. 2003, A&Ap, 397, 7
Lacerda, P., Jewitt, D., & Peixinho, N. 2008, AJ, Accepted
Licandro, J., Oliva, E., & Di Martino, M. 2001, A&A, 373, L29
Licandro, J., Campins, H., Hergenrother, C., & Lara, L. M. 2003, A&A, 398, L45
Licandro, J., di Fabrizio, L., Pinilla-ALonso, N., et al. 2006, A&A, 457, 323
Massey, P., Valdes, F., & Barnes, J. 1992, in A User's Guide to Reducing Slit Spectra with IRAF, http://iraf.noao.edu/iraf/ftp/iraf/docs/spect.ps.Z.
Merlin, F., Guilbert, A., Dumas, C., et al. 2007, A&A, 466, 1185
Moore, M., Donn, B., Khanna, R., & A'Hearn, M. 1983, Icarus, 54, 388
Nesvorny, D., & Roig, F. 2001, Icarus, 150, 104
Pinilla-Alonso, N., Brunetto, R., Licandro, J., & Gil-Hutton, R. 2007, A&A, 468, L25
Rabinowitz, D. L., Barkume, K., Brown, M. E., et al. 2006, ApJ, 639, 1238
Ragozzine, D., & Brown, M. E. 2007, AJ, 134, 2160
Santos-Sanz, P., Ortiz, J., Aceituno, F., et al. 2005, IAU Circ., 8577, 2
Schaller, E. L., & Brown, M. E. 2007, ApJ, 670, L49
Schmitt, B., Quirico, E., Trotta, F., & Grundy, W. M. 1998, Solar System Ices (Kluwer Academic Publisher)
Sill, G. T., Fink, U., & Ferraro, J. R. 1980, JOSA, 70, 724
Stevenson, D. J. 2004, Nature, 432, 681
Stern, A. 2002, AJ, 124, 2297
Strazzulla, G., & Johnson, R. 1991, in Comets in the Post-Halley era, ed. R. L. Newburn, Jr., M. Neugebauer, & J. Rahe (Netherlands: Kluwer Academic Publishers), 243
Strazzulla, G., Cooper, J. F., Christian, E. R., & Johnson, R. E. 2003, C.R. Phys., 4, 791
Tegler, S. C., Grundy, W. M., Romanishin, W., et al. 2007, A&A, 133, 526
Trujillo, C. A., Brown, M., Barkume, K. M., et al. 2007, ApJ, 655, 1172
Warren, S. G. 1984, ApOpt, 23, 1206
Zubko, V. G., Menella, V., Colangeli, L., & Bussoletti, E. 1996, MNRAS, 282, 1321